International Journal of Physics and Mathematical Sciences ISSN: 2277-2111 (Online)
An Open Access, Online International Journal Available at http://www.cibtech.org/jpms.htm
2019 Vol. 9 (4) October-December, pp. 1-9/Yuan and Wu
Research Article

THE BERNSTEIN OPERATIONAL MATRICES FOR INVERSION OF ABEL'S INTEGRAL EQUATION

Xia Yuan and Jieer Wu*
Department of School of Science, Jiangsu University of Science and Technology, Jiangsu 212003, China
**Author for Correspondence*: *wujieer@yeah.net*

ABSTRACT
In this paper, we focus on the numerical solution for Abel integral equation derived from the plasma diagnostics. To solve the Abel integral equation, we use a least squares fitted to a given discrete experimental data to represent the input function by nth Bernstein polynomials and reduce the solution of the integral equation to a set of numerical integrations by collocation method. Numerical simulations for this numerical scheme are performed and the obtained numerical results show the efficiency and accuracy of the proposed method.

Keywords: *Abel integral equation, Bernstein polynomials, least squares fitting method, Lagrange interpolating polynomial*

INTRODUCTION
The subject of this article is numerical solution of Abel's integral equation of the form

$$I(y)=2\int_y^1 \frac{g(r)r}{\sqrt{r^2-y^2}}dr,\ 0\le y\le 1,\ (with\ I(0)=0). \tag{1}$$

In Eq.(1), $I(y)\in L^2(0,1)$ represents a well behaved known data function, and $g(r)\in L^2(0,1)$ is the unknown function to be determined. Abel's integral equation (1) has many applications in various physical problems. For example in plasma diagnostics, $I(y)$ is an projected intensity function that can be measured only at a discrete set of data point from the outside of the source, while the physically important data $g(r)$ is the radial distribution of emission coefficient to be determined(Gueron *et al*.,1993, Pandey, *et al*.,2014, Deutsch *et al*.,1982). Although one can get the exact values of g(r) by using the analytical inversion of Eq.(1)

$$g(r)=\frac{-1}{\pi}\int_r^1 \frac{1}{\sqrt{y^2-r^2}}I'(y)dy, 0\le r\le 1, (\text{with } g(1)=0), \tag{2}$$

where the prime on I denotes differentiation with respect to y. Usually analytical solution (2) fails in practical application because the differential operation is an ill-posed problem and its solution does not depend continuously on the input data. In other words, the small errors in measured input data $I(y_i), i=0,1,2,...,m$ can be amplified by numerical differentiation and the g(r) is meaningless. Consequently in order to yield a stable solution of Eq.(2), many numerical methods have been developed. Some of these methods are derivative-free inversion method(Gueron *et al*.,1993, Deutsch *et al*.,1982, Deutsch *et al*.,1983), analytic spline Abel inversion method (Gueron *et al*.,1993), piece-wise cubic spline method(Deutsch,*et al*.,1983), low order interpolation methods(Edels,*et al*.,1962), least squares fit method(Freeman, *et al*.,1963, Freeman, *et al*.,1960, Cremers, *et al*.,1966), Gaussian basis-set expansion combined with Tikhonov regularization method(Dribinski, *et al*.,2002) for 2D Abel integral equation, orthogonal polynomials method with least squares fit(Minerbo, *et al*.,1969), Legendre wavelets expansion method(Shuiliang, *et al*.,2007), a simple analytic representation for experimental data method(Deutsch,1983), generalized Taylor-Stieltjes polynomial approximation method.
As an important mathematical approximation tools, the Bernstein polynomials are defined simply and can

represent many functions, therefore they were often used for solving integral equations and differential equations(Maleknejad, *et al*.,2011, Doha, *et al*.,2011, Mandal, *et al*.,2007, Maleknejad, *et al*.,2012). Furthermore, they are also used to approximate the solution of Abel's integral equation of the form(Sadri, *et al*.,2018, Jahanshahi, *et al*.,2015, Mohsen, *et al*.,2011, Singh, *et al*.,2009)

$$I(y)=\int_0^y \frac{g(r)}{\sqrt{y-r}}dr, 0\le y\le 1,$$

which is also known as singular Volterra integral equation of first kind.

In this paper we present a new method based on the Bernstein polynomials for the computation of emissivity $g(r)$ numerically by Eq.(2). This method is simple and effective since the numerical results $g(r_i), i=0,1,...,m$ can be obtained from a set of integrals. Some numerical experiments illustrate the stability of the method for the computation of $g(r_i)$ with various levels of noise on the input data $I(y_i), i=0,1,2,...,m$.

THE BERNSTEIN POLYNOMIALS AND FUNCTION APPROXIMATION

In this section we will recall the definition of Bernstein Polynomials and their properties(Maleknejad, *et al*.,2011). The Bernstein polynomials of *n*th degree are defined by

$$B_{i,n}(r)=\binom{n}{i}r^i(1-r)^{n-i}=\sum_{k=0}^{n-i}(-1)^k\binom{n}{i}\binom{n-i}{i}r^{k+i}, i=0,1,...,n, \tag{3}$$

where $\binom{n}{i}=\frac{n!}{i!(n-i)!}$ denotes the binomial coefficient. Eq.(3) are also called the Bernstein basis polynomials, which form a complete basis over interval [0,1]. From Eq.(3) we can find that $B_{i,n}(r)$ (i= 0,1,…,n) are positivity for all *t* in [0,1] and the sum $\sum_{i=0}^{n} B_{i,n}(r)$ equals to one. Consequently, we have $0\le B_{i,n}(r)\le 1$.

Bernstein polynomials have the following approximate properties(Khuri, *et al*.,2015). For a continuous or square integrable function $I(y)$ defined on [0, 1], we have

$$I(y)=\lim_{n\to\infty}\sum_{i=0}^{n} I(i/n)B_{i,n}(y), \tag{4}$$

and

$$I^{(r)}(y)=\lim_{n\to\infty}\sum_{i=0}^{n} I(i/n)B_{i,n}^{(r)}(y), r = 1, 2, . . .$$

Accordingly Bernstein polynomials yield an uniform approximation of the function $I(y)$ and its derivatives, which is beneficial for the approximation of derivative of $I(y)$.

SOLUTION OF ABEL'S INTEGRAL EQUATION

In this section we will discuss how to recover the unknown $g(r)$ by Bernstein polynomials.

In practice, $I(y)$ is often given as a set of discrete experimental data on points, $I_j=I(y_j)$, in which $y_j\in[0,1], j=0,1,...,m$ and $m>>n$. In order to use Eq.(2) to recover $g(r)$, we need to known the analytical expression of $I(y)$. This can be accomplished in advance by the Bernstein polynomials to fit the data $(y_j, I_j), j=0,1,...,m.$

Taking a truncated series of Eq.(4), an approximation of $I(y)$ can be written as

$$I(y)\approx \tilde{I}(y)=c_0B_{0,n}(y)+c_1B_{1,n}(y)+...+c_nB_{n,n}(y)=\Psi(y)^T C, \tag{5}$$

where

$C=(c_0,c_1,...,c_n)^T$,

$\Psi(y)=(B_{0,n}(y),B_{1,n}(y),...,B_{n,n}(y))^T$.

Eq.(5) can also be written as in matrix form:

$$\tilde{I}(y)=\left(1,y,y^2,...,y^n\right)\begin{pmatrix} d_{00} & 0 & 0 & ... & 0 \\ d_{10} & d_{11} & 0 & ... & 0 \\ d_{20} & d_{21} & d_{22} & ... & 0 \\ ... & ... & ... & ... & ... \\ d_{n0} & d_{n1} & d_{n2} & ... & d_{nn} \end{pmatrix}\begin{pmatrix} c_0 \\ c_1 \\ ... \\ c_n \end{pmatrix}=\left(1,y,y^2,...,y^n\right)DC, \tag{6}$$

where $D\in R^{n+1,n+1}$ and its elements $d_{i,j}=\begin{cases}(-1)^{j-i}\binom{n}{i}\binom{i}{j} & i\geq j, \\ 0 & i<j.\end{cases}$

The unknown vector C in Eq.(6) can be calculated by least squares fitting method of the form (5). Inserting the experimental data $(y_j,I_j), j=0,1,...,m$ in Eq.(6), we get

$$I_j=\left(1,y_j,y_j^2,...,y_j^n\right)DC,\ j=0,1,...,m. \tag{7}$$

Writing Eq.(7) in matrix form as

$$AC=I, \tag{8}$$

where matrix $A=YD$, and

$$Y=\begin{pmatrix} 1 & y_0 & y_0^2 & ... & y_0^n \\ 1 & y_1 & y_1^2 & ... & y_1^n \\ ... & ... & ... & ... & ... \\ 1 & y_m & y_m^2 & ... & y_m^n \end{pmatrix}\in R^{m+1,n+1},$$

$I=(I_0,I_1,...,I_{\mathrm{m}})^T$.

If the points y_j satisfies $y_0<y_1<...<y_m, m>>n$, then T is a matrix of rank $n+1$ and the unknown vector C can be solved by $C=(A^TA)^{-1}A^TI$. The desirable approximate $\tilde{I}(y)$ to $I(y)$ in Eq.(6) is known and the differentiation of $I(y)$ is given approximately as follows:

$$I'(y)\approx\tilde{I}'(y)=\left(0,1,2y\ ,...,ny^{n-1}\right)DC=\left(1,y,y^2,...,y^n\right)\begin{pmatrix} 0 & 1 & & & \\ 0 & 0 & 2 & & \\ 0 & 0 & 0 & \text{O} & \\ ... & . & . & . & \text{O} & n \\ 0 & 0 & 0 & . & . & 0 \end{pmatrix}DC$$

$$=\left(1,y,y^2,...,y^n\right)D_1DC.$$

Hence we obtain an approximate solution $g'(r)$ to analytical expression $g(r)$ as follows:

$$g(r)\approx\tilde{g}(r)=\frac{-1}{\pi}\int_r^1\frac{1}{\sqrt{y^2-r^2}}I'(y)dy=\frac{-1}{\pi}\int_r^1\frac{\left(1,y,y^2,...,y^n\right)}{\sqrt{y^2-r^2}}dyD_1DC$$

$$=\frac{-1}{\pi}\left(\int_r^1\frac{1}{\sqrt{y^2-r^2}}dy,\int_r^1\frac{y}{\sqrt{y^2-r^2}}dy,...,\int_r^1\frac{y^n}{\sqrt{y^2-r^2}}dy\right)\cdot D_1DC. \tag{9}$$

The integrals in the right hand of Eq.(9) can be calculated explicitly(Shuiliang,*et al.*,2007) by following integral:

$$\int_r^1 \frac{y^k}{\sqrt{y^2-r^2}}dy = i\frac{r^k}{2}\left(beta\left(\frac{1}{r^2},\frac{k+1}{2},\frac{1}{2}\right)-beta\left(1,\frac{k+1}{2},\frac{1}{2}\right)\right), \tag{10}$$

where

$$beta(z,p,q)=\int_0^z y^{p-1}(1-y)^{q-1}dy.$$

If only the values of $g(r_i)$ on a set of discrete points $r_i \in [0,1], i=0,1,...,m$ are desired, we can substitute $r=r_i$ in Eq.(9) to get the results. Note that for special point r=0, Eq.(10) is numerically impractical and $g(0)$ can be calculated by Lagrange interpolating polynomial with points ($(r_i, g(r_i)), i=1,2$):

$$g(0)=g(r_1)\frac{r_2}{(r_1-r_2)}+g(r_2)\frac{r_1}{(r_2-r_1)}.$$

NUMERICAL ILLUSTRATIONS

In this section, we give two examples for computation of emission coefficient functions as follows:

(1) $g_1(r)=\frac{4}{3}\sqrt{\pi}e^{-(\pi r)^2}$,

(2) $g_2(r)=(1-r^2)^2(1+12r^2)$.

The corresponding simulated input data $I_k(y_j), k=1,2$ are calculated from Eq.(1) for a given $g_k(r), k=1,2$ by numerical integration method with m=30 and $y_j=j/m, j=0,1,2,...,m$. The task here is to calculate the values of $g_k(r), k=1,2$ at nodes $r_i=i/m, i=0,1,...,m$ by the proposed method. The accuracy of the results is given by the mean standard deviation formula(RMS):

$$RMS=\left(\frac{1}{m+1}\sum_{i=0}^{m}\left|g_k^{\delta}(r_i)-g_k(r_i)\right|^2\right)^{\frac{1}{2}}.$$

To test the stability of the method, we add the random error to the simulated $I_k(y_j)$ data, i.e. replacing $I_k^{-l}(y_j)=I_k(y_j)(1+\rho\times10^{-l}),(k=1,2,l=1,2,3)$ with $I_k(y_j)$, where ρ is a normal distribution with mean 0 and standard deviation 1 and l is an error level. Note that $l=0$ means that $I_k^{-l}(y_j)$ is an error free input $I_k(y_j)$. The recovered emission coefficient is denoted $g_k^{-l}(r_i)$.

All the numerical results are obtained with MathCAD2001.

Case 1. Consider the Eq.(1) with $g_1(r)=\frac{4}{3}\sqrt{\pi}e^{-(\pi r)^2}$. Fig.1 summarizes the simulated input data $I_1^{-l}(y_j)$ with $j=0,1,...,m$ and $m=30$. The figures of the recovered $g_1^{-l}(r_i)$ by 5th Bernstein polynomials are plotted in Fig.(2), while the figures of the $g_1^{-l}(r_i)$ recovered by 10th Bernstein polynomials are plotted in Fig.(3). In panel(a) of Figs.2,3, we see the reconstruction of $g_1(r)$ is excellent for the noise level $l=0$. Panel(b)-(d) of Figs.2,3 show the recovered $g_1^{-l}(r)$ with $l=1,2,3$ in the case of noisy input data(see Fig.1bcd). In this example the reconstruction shown in Panel(b)-(d) of Figs.2,3 exhibit the good stability of the inversion algorithm, i.e. the dotted line(recovered $g_1^{-l}(r)$) fits well to the solid line(exact $g_1(r)$) as the error level decreases.

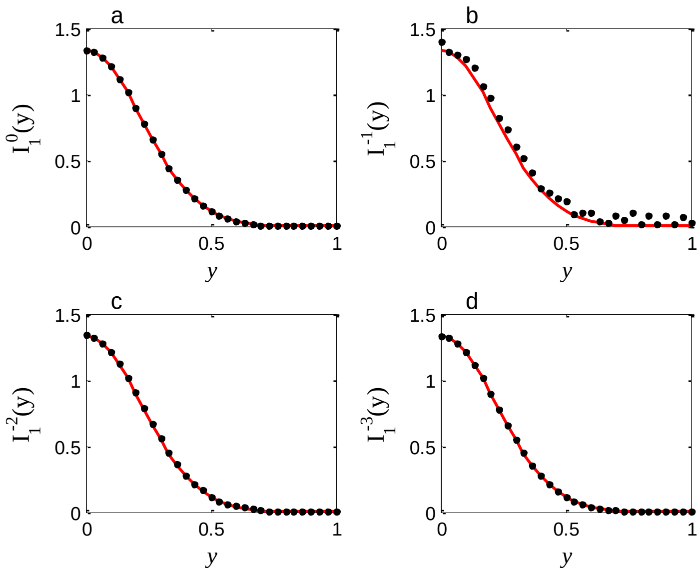

Fig.1 The input data $I_1^{-l}(y_j), j=0,1,\ldots,30, l=0,1,2,3$ (dotted lines) and the exact input data function $I_1(y), y\in[0,1]$ (solid lines)

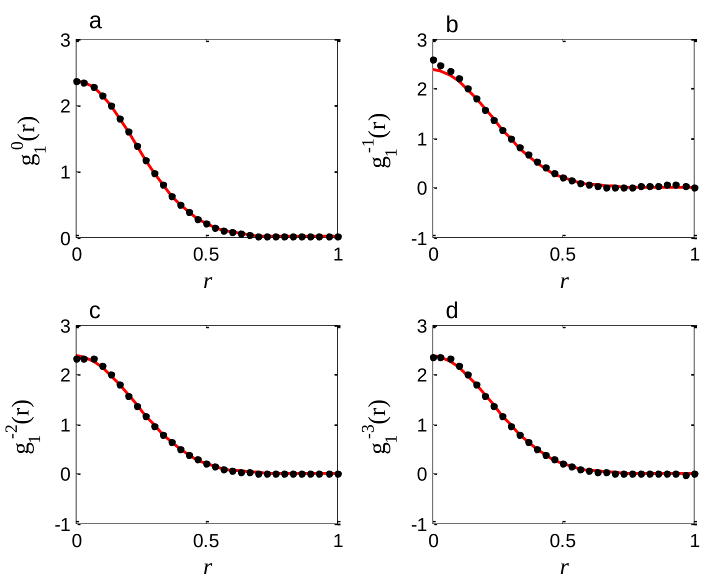

Fig.2 The recover $g_1^{-l}(r_i), i=0,1,\ldots,30$ (dotted lines) with $l=0,1,2,3$ by 5th Bernstein polynomials and the exact $g_1(r), r\in[0,1]$ (solid lines)

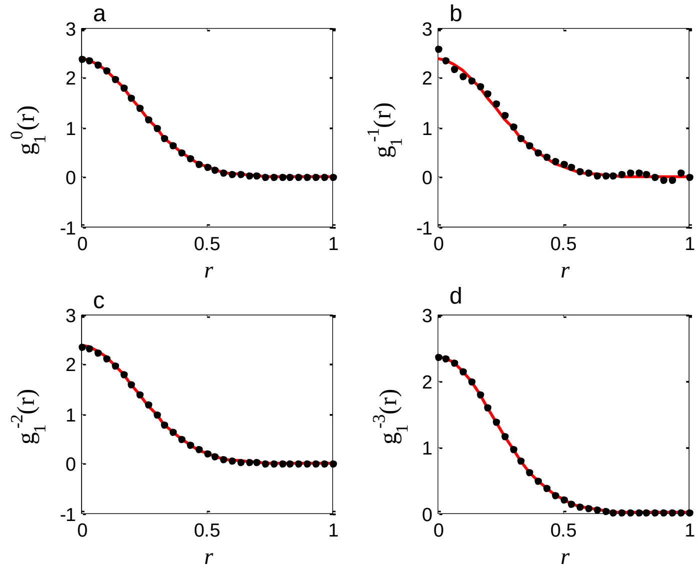

Fig.3 The recover $g_1^{-l}(r_i), i=0,1,...,30$ (dotted lines) with $l=0,1,2,3$ by 10th Bernstein polynomials and the exact $g_1(r), r\in[0,1]$ (solid lines)

Case 2. In this example we consider the Eq.(1) with $g_2(r)=(1-r^2)^2(1+12r^2)$. The simulated input data $I_2^{-l}(y_j), l=0,1,2,3$ with $j=0,1,...,m$ and $m=30$ are plotted in Fig.4 respectively. The results recovered by 5th and 10th Bernstein polynomials are shown in Fig.5 and Fig.6 respectively. Panel(a) of Figs5,6 refer to the case $l=0$ (i.e. error free), whereas Panel(b)-(d) of Figs 5,6 exhibit the results in the case of input data contaminated with error levels $l=0,1,2,3$. From Figs.5,6, we can clear see that the proposed method works well and the disagreements between the exact solution(solid line) and the numerical solution(dotted line) are getting reduced as we decrease the error level l.

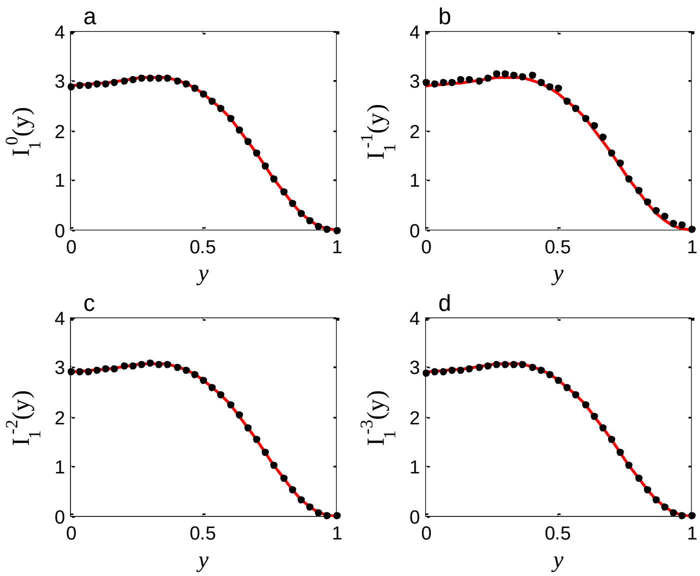

Fig.4 The input data $I_1^{-l}(y_j), j=0,1,...,30, l=0,1,2,3$ (dotted lines) and the exact input data function

$I_1(y), y\in[0,1]$ (solid lines)

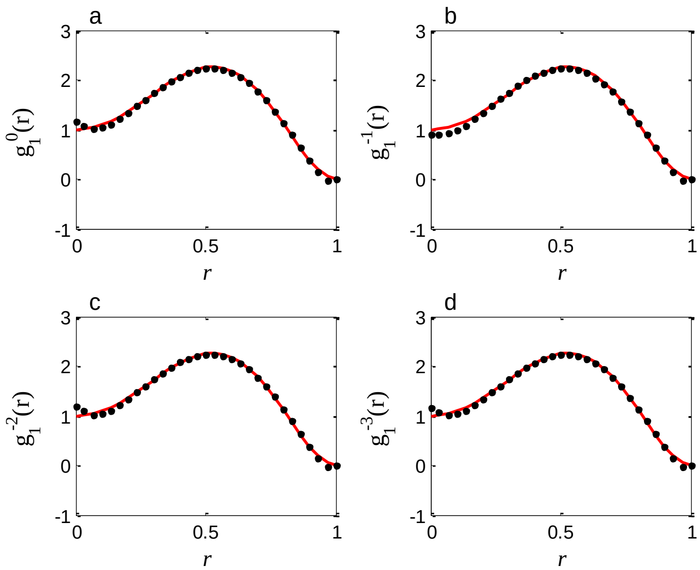

Fig.5 The recover $g_1^{-l}(r_i), i=0,1,...,30$ (dotted lines) with $l=0,1,2,3$ by 5th Bernstein polynomials and the exact $g_1(r), r\in[0,1]$ (solid lines)

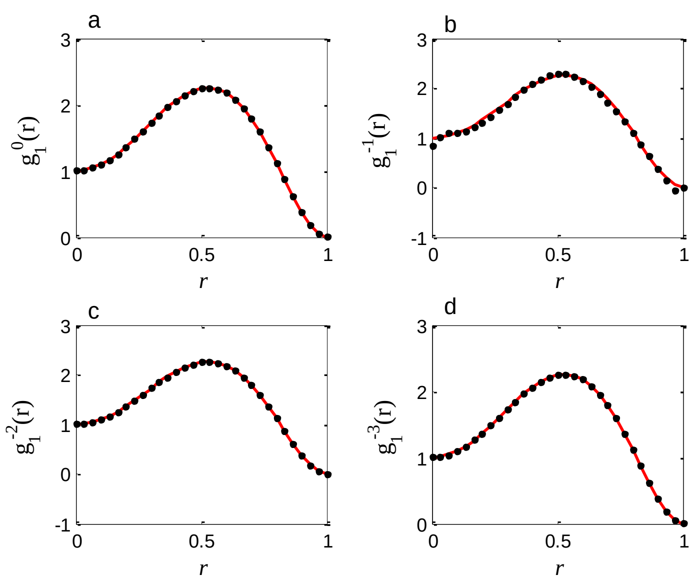

Fig.6 The recover $g_1^{-l}(r_i), i=0,1,...,30$ (dotted lines) with $l=0,1,2,3$ by 5th Bernstein polynomials and the exact $g_1(r), r\in[0,1]$ (solid lines)

Finally the RMS obtained with our method for these two examples, using 5^{th} and 10^{th} Bernstein polynomials for input data $I_1^{-l}(y_j), j=0,1,...,30, l=0,1,2,3$, are given in Table1. For both cases, we can find that the accuracy increases rapidly upon increasing the degree of Bernstein polynomials. Further, for the fixed degree of Bernstein polynomials, we also can see that the decrease of RMS on decreasing the error level.

Table 1. RMS for sets of the recovered $g_1^{-l}(r_i), i=0,1,\ldots,30$ **bwith different error level** l **.**

	Case 1		Case 2	
	n=5	n=10	n=5	n=10
$l=0$	0.0151	0.0009	0.0439	0.0008
$l=1$	0.0344	0.1569	0.0513	0.0511
$l=2$	0.0159	0.0085	0.0474	0.0073
$l=3$	0.0152	0.0011	0.0437	0.0016

CONCLUSIONS

We have presented a new method for the computation of the inverse Abel integral equation. The solution is expressed in terms of the sum of nth Bernstein polynomials and can be computed through a series of numerical integrations. This makes the method particularly appropriate for the case that the input experimental data are given on (even nonequispaced) points. Two examples have been presented and the results show the stability and the accuracy of the method for the reconstruction of emission coefficient with different noise of error level on the data.

REFERENCES

Cremers C J, Birkebak R C (1966). Application of the Abel Integral Equation to Spectrographic Data. *Applied Optics* **5**(6) 1057-1064.

Deutsch M, Beniaminy I (1982). Derivative-free inversion of Abel’s integral equation. *Applied Physics Letters* **41**(1) 27-28.

Deutsch M, Beniaminy I (1983). Inversion of Abel’s integral equation for experimental data. *Journal of Applied Physics* 54(1) 137-143.

Deutsch M(1983). Abel inversion with a simple analytic representation for experimental data. *Applied Physics Letters* **42**(3) 237-239.

Dribinski V, Ossadtchi A, Mandelshtam V A, H Reisler (2002). Reconstruction of Abel-transformable images: The Gaussian basis-set expansion Abel transform method. *Review of Scientific Instrument* **73**(7) 2634-2642.

Doha E H, Bhrawy A H, Saker M A (2011). Integrals of Bernstein polynomials: An application for the solution of high even-order differential equations. *Applied Mathematics Letters* **24**(4) 559-565.

Edels H, Hearne K, Young A (1962). Numerical Solutions of the Abel Integral Equation. + 62-75.

Freeman M P, Katz S (1960). Determination of the Radial Distribution of Brightness in a Cylindrical Luminous Medium with Self-Absorption. *Journal of the Optical Society of America* **50**(8) 826-830.

Freeman M P, Katz S (1963). Determination of a Radiance-Coefficient Profile from the Observed Asymmetric Radiance Distribution of an Optically Thin Radiating Medium. *Journal of the Optical Society of America* **53**(10) 1172-1179.

Gueron S, Deutsch M (1993). A Fast Abel Inversion Algorithm. *Journal of Applied Physics* 75(9) 4313-4318.

Jahanshahi S, Babolian E, Torres D F, Alireza Vahidi (2015). Solving Abel integral equations of first kind via fractional calculus. *Journal of King Saud University - Science* **27**(2) 161-167.

Khuri A I, Mukhopadhyay S, Khuri M A (2015). Approximating moments of continuous functions of random variables using Bernstein polynomials. *Statistical Methodology* 37-51.

Mandal B N, Bhattacharya S (2007). Numerical solution of some classes of integral equations using Bernstein polynomials. *Applied Mathematics and Computation* **190**(2) 1707-1716.

Maleknejad K, Hashemizadeh E, Ezzati R (2011). A new approach to the numerical solution of Volterra integral equations by using Bernsteins approximation. *Commun Nonlinear Sci Numer Simulat*16

647–55.
Mohsen Alipour, Davood Rostamy (2011). Bernstein polynomials for solving Abel's integral equation. *The Journal of Mathematics and Computer Science* **3**(4) 403 - 412.
Maleknejad K, Hashemizadeh E, Basirat B (2012). Computational Method Based on Bernstein Operational Matrices for Nonlinear Volterra-Fredholm-Hammerstein Integral Equations. *Communications in Nonlinear Science and Numerical Simulation* **17**(1) 52-61.
Pandey R K, Suman S, Singh K K, Om P Singh (2014). An approximate method for Abel inversion using Chebyshev polynomials. *Applied Mathematics and Computation* 120-132.
Minerbo G N, Levy M E (1969). Inversion of Abel's Integral Equation by Means of Orthogonal Polynomials. *SIAM Journal on Numerical Analysi* **6**(4) 598-616.
Shuiliang Ma, Hongming Gao, Guangjun Zhang, Lin Wu (2007). Abel inversion using Legendre wavelets expansion.*Journal of Quantitative Spectroscopy & Radiative Transfer* 107 61-71.
Sadri K, Amini A, Cheng C (2018). A new operational method to solve Abel's and generalized Abel's integral equations. *Applied Mathematics and Computation* 49-67.
Singh V K, Pandey R K, Singh O P (2009). New stable numerical solutions of singular integral equations of Abel type by using normalized Bernstein polynomials. *Applied Mathematical Science* 3(5) 241–255.
Xianfang Li, Li Huang, Yong Huang (2007). A new Abel inversion by means of the integrals of an input function with noise. *Journal of Physics A* **40**(2) 347-360.